Applied Chemical Engineering (2026) Volume 9 Issue 4 ISSN: 2578-2010 (O)
doi: 10.59429/ace.v9i4.5980

RESEARCH ARTICLE

Nanocomposite (GO/Zn + Fe) is made by preparing nanometals utilizing plasma technique, and it is used as a sensor for H2S gas

Ibrahim Hammadi Frhan [1*], Ahmed Mohammed Alrawi [2], Huthaifa. M. Yaseen [2], Marwan Abdulaziz Hassan [3]

[1] *Ministry of Education, Directorate of Anbar Education, Anbar, Iraq*

[2] *College of Education, University of Fallujah, Anbar, Iraq*

[3] *University of Anbar, Anbar, Iraq*

***Corresponding author:** Ibrahim Hammadi Frhan, Ibrahim.hum69@gmail.com

ABSTRACT

The nanocomposite was created and prepared in a process aimed at creating highly efficient nanosensors and adopting the necessary tests for that. The plasma technique was used to prepare the (Zn) and (Fe) nano-metals. These nano-metals were identified by FAAS technique to find out their concentrations. It was also diagnosed using FTIR, UV-Vs, FESEM, and XRD techniques. In addition to the preparation of graphene oxide by Hummer method to make a nanocomposite of oxide and nanometals with a mixing ratio of 10:1:1. Gaseous sensitivity tests were carried out on the (GO/Zn+Fe) nanocomposite towards H2S gas, and it gave good sensitivity to the gas. The process of mixing two metals with graphene oxide to create this composite has proven to be more successful than using iron alone.

Keywords: Nano, Gas sensor Nanoparticle, Plasma, Graphene Oxide and sensitivity

ARTICLE INFO

Received: 13 April 2026
Accepted: 16 June 2026
Available online: 03 November 2026

COPYRIGHT

Copyright © 2026 by author(s).
Applied Chemical Engineering is published by Arts and Science Press Pte. Ltd. This work is licensed under the Creative Commons Attribution-NonCommercial 4.0 International License (CC BY 4.0).
https://creativecommons.org/licenses/by/4.0/

1. Introduction

Nanocomposites are defined as "multiphase materials where one or more of the phases have at least one dimension of order 100nm or less" by Cammarata (2006). Similar to traditional composites, he noted. The characteristics of nanocomposites may exhibit individual synergistic [1]. The composite's many parts come together to give it its unique characteristics. For thousands of years, composite materials have been used by humans for a variety of applications. The fact that graphene oxide and its derivatives are significant generators of light, heat, and gas sensitivity bodes well for the material's future [2]. An essential factor in identifying the characteristics of matter is its dimensionality. The formation of unique characteristics and the regulation of the structure at the nanoscale are largely dependent on a material's nanostructure. Thus, nanotechnology is a very promising subject for the twenty-first century that is predicted to completely transform the applications of technology in semiconductors, energy storage, organic and inorganic materials, and biotechnology [3].

The controlled manipulation of materials with at least one dimension smaller than 100 nm is referred to as "nanotechnology." [4]. In order to establish novel material characteristics that may be used to easily construct procedures for the manufacturing of consumer goods, high-performance materials, electronic gadgets, and biomedical items, this technology aims to merge chemistry, physics, materials science,

and biology. Global socioeconomic advantages, enhanced quality of life, and rapid scientific advancement are anticipated with the commercialization of nanotechnology [5].

Graphene is a two-dimensional (2D) sheet of atomically thin sp2 carbon atoms arranged in a honeycomb pattern. Numerous positive attributes have been demonstrated by it, including strong mechanical strength [6], amazing qualities such as electrical conductivity and molecular barrier capabilities. For these reasons, creating polymer-based nanocomposites by incorporating graphene into polymers has been the aim of innumerable research projects [7]. Graphite oxide, which is made up of several stacked layers of graphene oxide (GO), is produced when graphite is oxidized in protonated fluids. In addition to hydroxyl (-OH), alkoxy (C–O–C), carbonyl (C—O), carboxylic acid (–COOH), and other oxygen-based functional groups, graphene and GO have a similar hexagonal carbon structure [8, 9]. In contrast to graphene, graphite oxide (GO) is hydrophilic, which makes it relatively easy to prepare suspensions in water or organic solvents. Highly oxidized forms of GO are electric insulators with a bandgap of approximately 2.2 eV. GO can be synthesized by first oxidizing graphite to graphite oxide, then exfoliating this graphite oxide into GO. The properties of the material are strongly dependent on the method of synthesis [10]. Air pollution resulting from the industrial discharge of hazardous gases such CO_2, CO, NO_2, H_2S, and NH_3 is one of the largest risks to the environment. Owing to the oxygen groups adorning the edges and basal planes, GO can engage covalently or noncovalently with a variety of molecules. This led to the beginning of its scientific significance and its introduction into a number of industrial, medical, and agricultural domains [11]. GO can be utilized as a catalyst in industrial processes to transform hazardous gasses. Direct use, catalytic procedures for gas conversion, or gas capture and storage are some ways to get rid of these dangerous gases. Graphene oxide is a graphite derivative consisting of one or more thin layers of carbon atoms containing oxygen-rich functional groups. It is characterized by its dispersibility and solubility in water due to the presence of polar functional groups. These groups provide it with a large surface area for adsorption and chemical reactions. [12]. Recent technological advancements require a novel multifunctional nanomaterial. Because of their special qualities, nano metal oxide/porous carbon composites are generally predicted to meet the aforementioned thrust. Because they are widely used as adsorbents, photocatalysts, and sensors with better qualities, nanosized metal oxides are far more interesting than bulk materials. In addition to being used, they pollute the environment [13]. A new strategy for creating metal oxide carbon composites, which stable metal oxide in carbon matrix and prevent polluting of the environment, has emerged to counteract this. An additional benefit is the simple process for recycling the materials [14]. Carbon's low energy makes it unsuitable for use in energy storage devices, just as metal oxide's low density and instability. Researchers have combined metal oxides with carbon materials to create metal oxide carbon composite in an effort to overcome the drawbacks of both carbon and metal oxide and to enhance its properties [15]. The incorporation of nano-metals into graphene oxide is crucial for enhancing its electrical and thermal conductivity, as well as for enabling it to sense gases and interact with other materials. This is accomplished by adding nanometals to the spaces between the molecules of graphene oxide, greatly enhancing its characteristics [16].

The most common use of nanomaterials and nanoparticles in sensing applications are when they are attached to organic or inorganic molecules as nanowires [17]. Enhancing physical characteristics of a nanowire, such as its electrical conductivity and impedance, by joining complimentary nanoparticles to create powerful composites, has been a popular approach in device engineering to greatly increase the device response [18]. Certain materials can also respond to light, and they can be used in conjunction with nanoparticles to create sensing devices. The degree of change brought about by the adduct material will determine how quickly charge and electron transfer efficiency increase. Additionally, adding nanoparticles to sensor surfaces will enhance their electrochemical characteristics. Higher signal-to-noise ratios and low background current are examples of these enhancements. Biosensors have also been made using a variety of metallic nanoparticles, such as

nickel (Ni), iridium (Ir), platinum (Pt), iron (Fe), cobalt (Co), copper (Cu), nickel (Ag), and others, either alone or in composite form. [19].

2. Materials and Methods

The Hammers method was used to convert graphite into graphene oxide. The components that are used are 97 percent pure $NaNO_3$, $KMnO_4$, and 98% pure H_2SO_4. Using the plasma process, nonmetals were also produced from their chloride salts. The approach utilizes argon gas and 5500 V of power.

2.1. Preparation of graphene oxide

Graphene oxide was prepared from graphite using the Hummers process. A 1000 mL beaker containing 96 mL of concentrated sulfuric acid (H_2SO_4) is cooled using an ice bath. Two grams of graphite, one gram of sodium nitrate ($NaNO_3$), and six grams of potassium permanganate ($KMnO_4$) are added to the reaction flask.[20]. Potassium permanganate should be added gradually because it raises the temperature. It is important to maintain the reaction's temperature below 10°C. The mixture's color will shift from black to green after two hours of continuousstirring (shown in Figure 1 -A). After being removed from the ice bath, the liquid is placed on a hotplate and stirred continuously for 36 hours at a temperature between 30 and 40°C. As seen in Figure 1-B, the color shifts from green to a brownish yellow hue. In order to prevent the temperature from rising, the reaction mixture is subsequently submerged in an ice bath once more. Next, add the water a little at a time while stirring constantly until the mixture reaches 500 ml. For two hours, the mixture of 5 mL of 30% hydrogen peroxide (H_2O_2) is added gradually and stirred continuously. We see that the color shifts from light brown to dark brown or reddish brown (as in Figure 1- C). First, after leaving the mixture for 24 hours, the top layer is separated from the precipitate by centrifugation at 6000 R/S for 15 minutes (as shown in Figure 1-D). Figure 1-E shows the brownish-black hue of the precipitate, while Figure 2 shows the yellowish-orange color of the filtrate. After the separation process, a 10% hydrochloric acid (HCl) solution is used to wash the precipitate, or graphene oxide, three times.

Until the graphene oxide precipitate achieves a steady pH function, it is washed several times with deionized water. The components are separated using a centrifuge following each washing step. To remove the water, the precipitate is dried in a drying oven for 24 hours at 60°C. To get rid of any remaining impurities, wash with ethanol next. To obtain a powder, the precipitate is completely treated. FTIR analysis is performed on a sample to diagnose graphene oxide. The procedure of preparation is iterated multiple times till the target weight is attained.

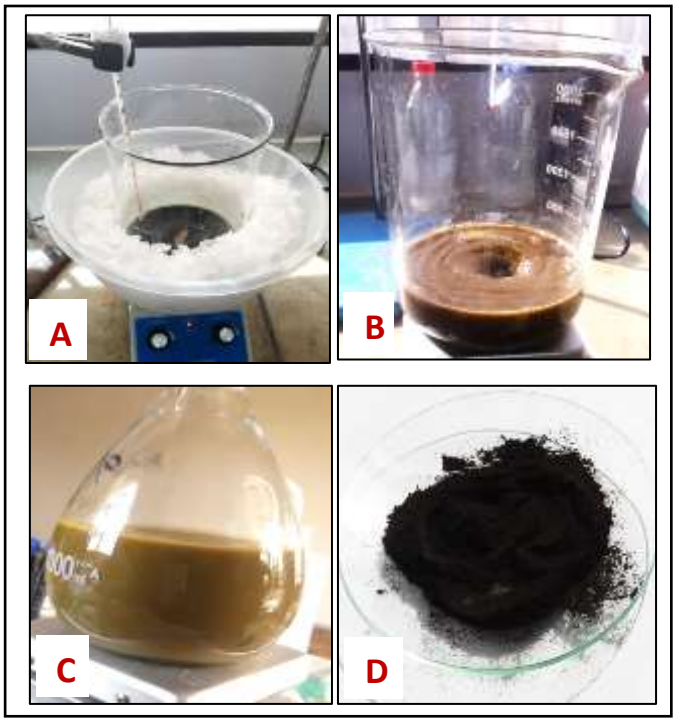


Figure 1. A representing the *first reaction step*, and the color turning green, B representing the *second reaction step*, and the color turning brown after 36 hours, C representing the *addition of H_2O and H_2O_2*, and D representing the *GO precipitate*.

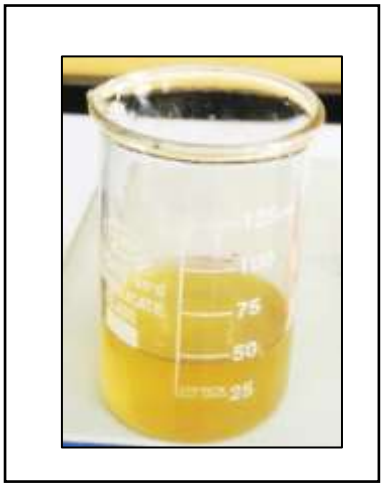


Figure 2. Demonstrates the color of the filtrate used to prepare graphene oxide.

2.2. How to use plasma to prepare metal nanoparticles

One of the key techniques for isolating metallic nanoparticles from their salts is the plasma method. [21]. There is a voltage of 5500 volts used. The flow rate of argon gas is fixed at 2 cm^3/s. (10 bar) is the pressure outside the gas bottle. Zinc chloride ($ZnCl_2$) and iron (III) chloride ($FeCl_3$) are the materials that have been prepared. Using a 500 ml volumetric flask, prepare concentrations of 1000 ppm or 2000 ppm for each of the metal salts. From the volumetric flask made with the metal salts, 40 ml is taken and put into a 75 ml beaker. Furthermore, a controller is positioned beneath the hotplate to raise and lower the system, and the beaker is set on the hotplate for stirring. The prepared solution is filled with the negative cell electrode, which is fixed one centimeter below the solution's surface. Attached to the capillary tube for argon gas is the positive electrode, which has a diameter of 2 mm. Additionally, the capillary tube is one centimeter from the solution's surface. The voltaic and gas apparatus is opened to produce plasma, which is continuously applied to the solution.The color shift of the solution indicates the transition, which happens over a few minutes. This alteration suggests

that metal nanoparticles are forming. Until the prepared solution in the volumetric flask runs out, this step is repeated multiple times. When the plasma is present, the solution's temperature doesn't go above 45 °C. The transformation of iron and zinc into nanoiron and nanozinc is shown in Figure (3). The color of the metal prior to conversion is represented by number 1 in the figure, and the color of the nano-metal following conversion is represented by number 2. These quantities of each element are collected and separated using a centrifuge set to 10,000–12,000 R/m. The precipitate is removed and mixed with the right volume of water (5 milliliters). After obtaining the required quantities of metallic nanoparticles, samples are taken from them for the purpose of examination UV, XRD, FESE.

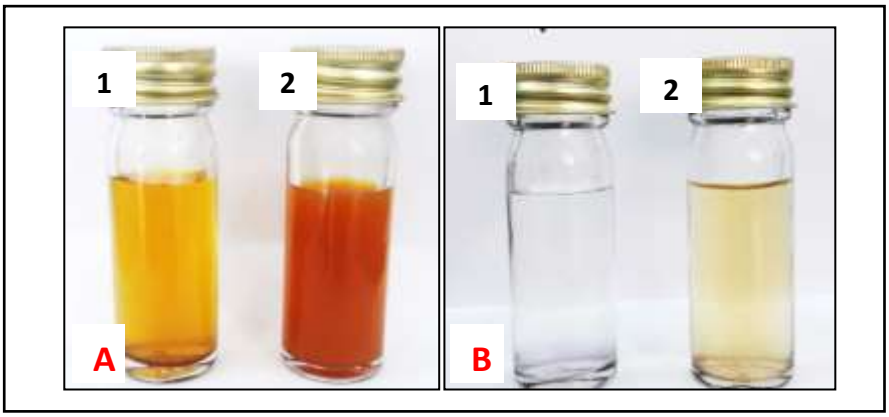


Figure 3. Symbolizes the formation and color shift of MNPs. (A) Shows how FeNPs and (B) ZnNPs form.

2.3. Preparation of Composites

Utilizing the Hummer technique to prepare the graphene oxide and the plasma method to convert its chlorides into metal nanoparticles. The preparation process for the nanocomposites is as follows: Deionized water is added to graphene oxide (GO), which is prepared at a concentration of 1000 ppm with a weight of 1 g of GO, in a volumetric flask with a 1000 ml capacity. A 10:1 ratio is used to mix GO/Fe+Zn NPs (1000 ppm of GO to 100 ppm of FeNPs and ZnNPs). Following the preparation of 10 ml of graphene oxide, the volume required is determined by utilizing deionized water to create 10 ml, while accounting for the stock's metal concentration and the target concentration of 100 ppm. In a glass volumetric vial, GO is mixed with FeNPs and ZnNPs (Composites) and heated to 30-35 °C for 48 hours while being continuously stirred. After that, the mixture (composites) undergoes an ultrasonic treatment for 15 minutes.

2.4. GO/Fe+Zn NPs gas sensing method

The composite sample is placed on silicon slides. These slides are completely cleaned of any contaminants using solvents like methanol, ethanol, and isopropanol. Dropper deposition is used on slides with a thickness of 22 nanometers and an area of 50 micrometers. The second step is to create the sample electrodes so that they may be transferred to the resistance measuring device. The samples are then individually put within a sealed system that only permits gasses to exit through pre-designated apertures. This device features an externally controllable electrical heat source with a temperature range of 0 to 200° C [22]. In order to perform the necessary computations, the temperature is altered and the resistance is measured at each temperature after the gas is pumped into the system at a specified pressure.

3. Results and Discussion

2.1. FT-IR analysis of GO and GR

The water solubility test results for GO and its spread are good compared to graphite (4). It not only confirms the FTIR measurement but also the transformation of graphite into graphene oxide. Between 600

and 4000 cm^{-1} in wavelength, elastic and bending bands were seen using graphene oxide and graphite FTIR spectra. The GO spectrum is shown in FT-IR Fig. (5-A). A broad and strong band that indicated the stretching vibration of the (C-OH, COOH) and H2O residue emerged at 3401.4 cm^{-1}. The unoxidized graphitic domain, which is a part of the aromatic rings' (C=C) group stretching beam, was identified as the source of the signal at 1587 cm^{-1}, as illustrated in figure 5-B. The locations of the two bands that corresponded to (C-O) stretching were 1400.5 cm^{-1} and 1221.78 cm^{-1} [23]. The (O-H) bending vibration of (COOH) groups can be used to calculate the number of COOH groups. Vibration was applied to alkoxy (C-OH) groups at 1060.18 cm^{-1}. Furthermore, a beam at 1716 cm^{-1} in the spectrum was found to be part of the stretching beam of group C = 0, indicating the synthesis of graphene oxide. Additionally, a broad, overlapping beam at 1186 cm^{-1} was seen; this beam is associated with (C-C), (C-O-C) epoxy. Furthermore, the band at 1721 cm^{-1} may be related to ketones or quinone in addition to the carbonyl group stretching vibration of (COOH) that is positioned at the borders. [24].



Figure 4. Comparison of the water solubility of graphite and graphene oxide.

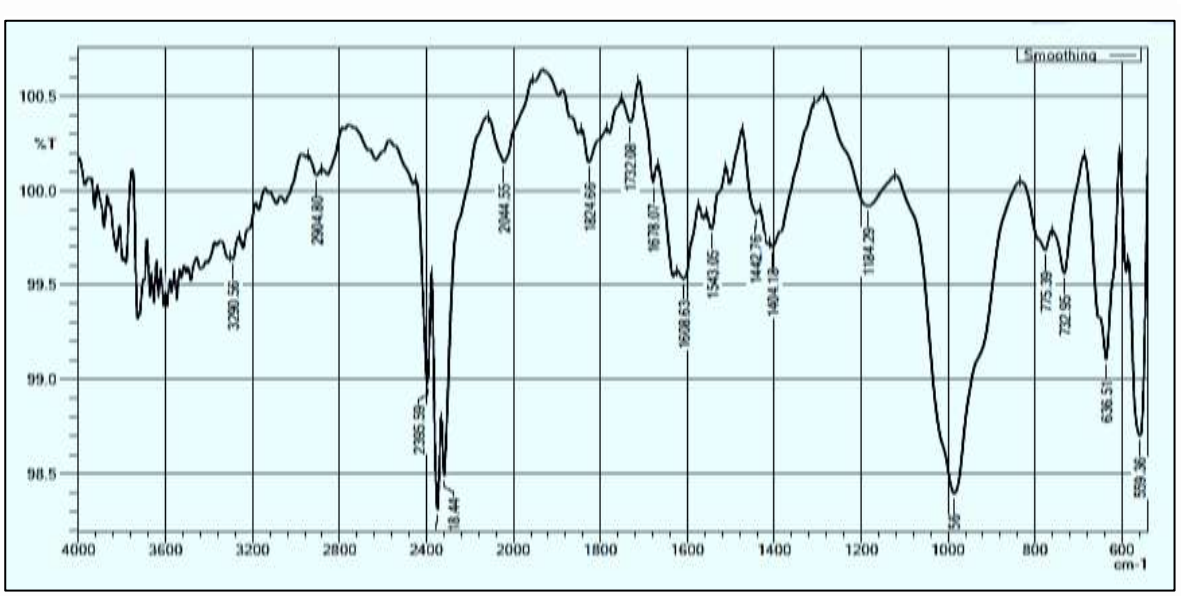


Figure 5-A. shows the graphene oxide FTIR spectrum.

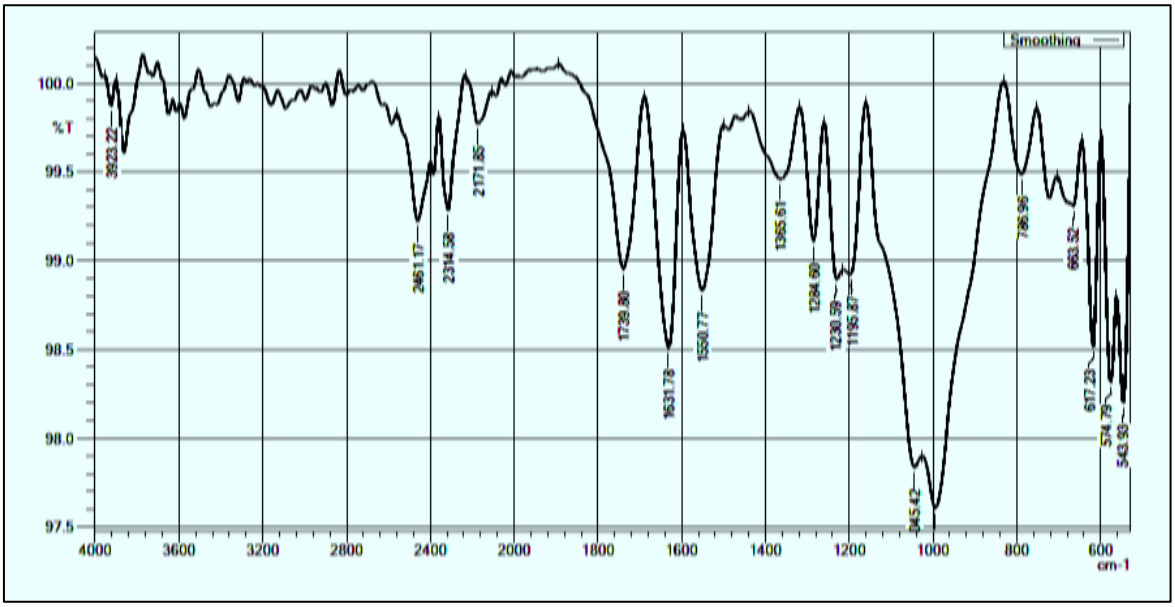


Figure 5-B. displays the graphite FTIR spectrum.

3.2. Using a UV-visible spectrophotometer for analysis

Studies are being done on ZnNPs and FeNPs. The absorption spectrum of nanoparticles formed in the 200–800 nm wavelength range was assessed with a resolution of 1 nm using a JASCO V 650 spectrophotometer. UV-Vis spectra of ZnNPs are shown in (Figure 6-B). The polydispersed nature of the nanoparticles was demonstrated by the large SPR band. The presence and synthesis of ZnNPs were indicated by a slight shift to the long wavelength region and a broadening of the SPR band at 280 nm. When particle size increased, SPR predominated in the optical absorption spectra of metal NPs, which shifted to longer wavelengths. Plasmon absorption in cobalt nanoclusters was influenced by surface-adsorbed species, dielectric medium, and particle size.

Furthermore, iron nanoparticle absorption peaked in the UV spectrum at a wavelength of 341 nm [25]. The absorption peak of iron nanoparticles is seen in (Figure 6-A) in the UV-VIS spectrum. UV-visible spectroscopy is one of the most widely used techniques for the structural characterization of FeNPs.

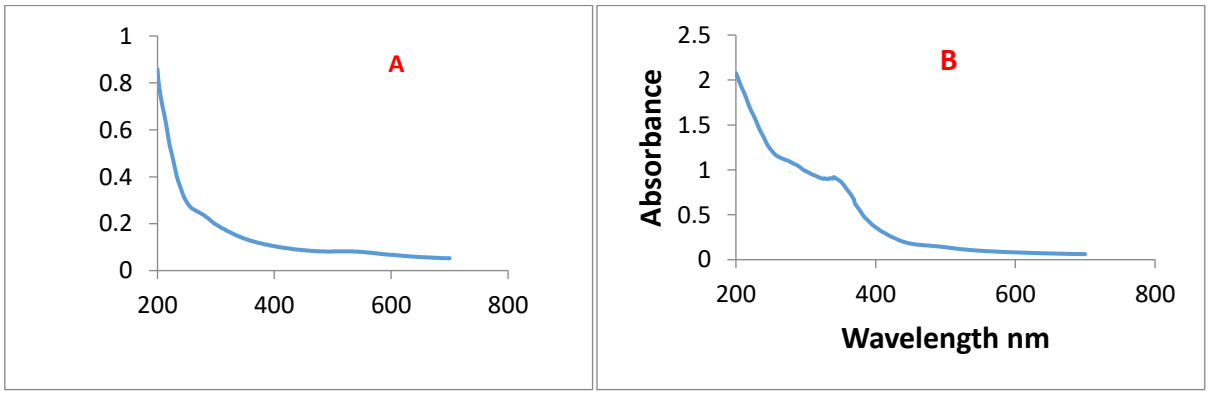


Figure 6. UV-*vis spectrum* of A- ZnNPs and B- FeNPs.

3.3. Field emission scanning electron microscope (FE-SEM)

One method for examining the surface morphology of materials is the (FE-SEM) method. The electrons are emitted from an accelerating emission source inside a high vacuum column by the ray beam, which is then focused on the sample by passing the electron beam through an electromagnetic lens. Consequently, a variety

of high-energy electron types are reflected. An elastic collision that occurred deep within the sample is what caused the high. The secondary electrons are produced by an inelastic collision on or near the sample's surface, and they are subsequently collected by the detector to create an image of the sample's surface. In order to produce a high-resolution image with a resolution of up to one nanometer, selecting the appropriate acceleration voltage is crucial. Using this method, the nano-diameters of graphene oxide were measured and found to be between 24 and 35 nm. As an alternative, they resemble stacked nanosheets. FE-SEM images of graphene oxide are presented in Figure 7.

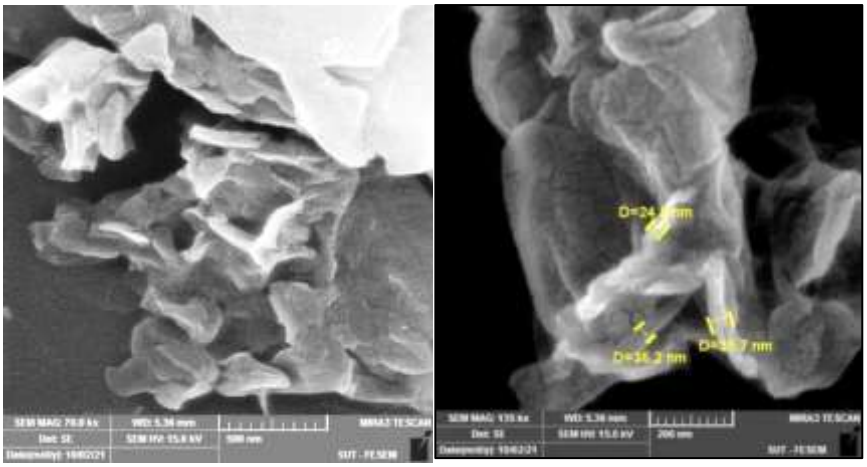


Figure 7. Graphene oxide FE-SEM images are displayed.

Figure (8) shows FE-SEM images of iron nanoparticles, which are big aggregates that resemble quantum dots, that were made from iron chloride (FeCl3) using a plasma method. Regarding the zinc nanoparticles, they were distinct shaped nanosheets that were superimposed. Zinc nanoparticle (ZnNP) FESM images are shown in Figure (9).

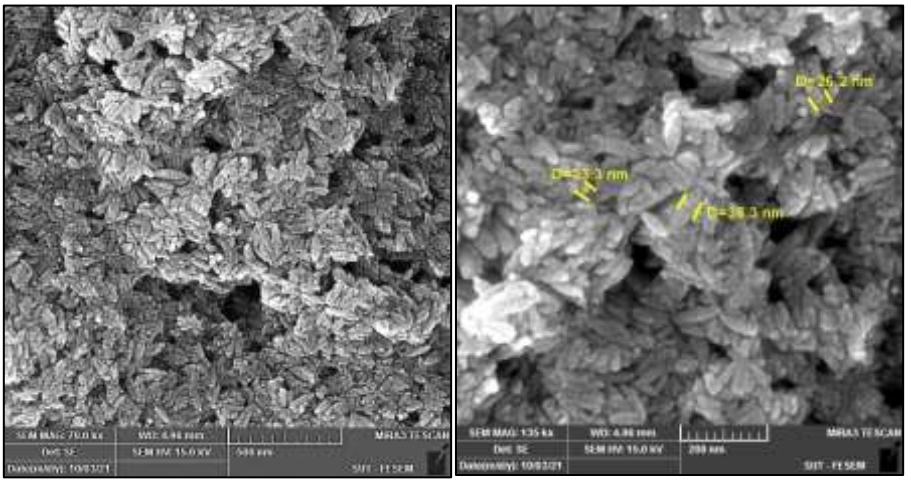


Figure 8. Represents FE-SEM images of *Iron nanoparticles*.

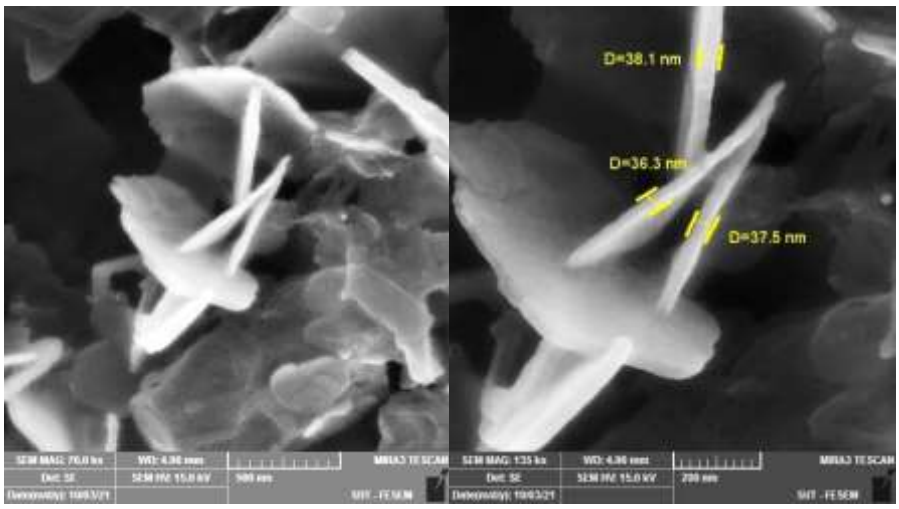


Figure 9. Represents FE-SEM images of *Zinc nanoparticles*.

3.4. Characterization of GO/Fe+Zn nanoparticles

The findings show that by introducing metallic nanoparticles like iron and zinc into the spaces between GO particles, GO/Fe+ZnNPs can provide good surface properties. These GO-containing particles would give the composite favorable characteristics like increased gas response and surface resistance to outside influences[26].

3.5. Analysis of XRD

GO nanoparticles were subjected to XRD analysis using a PANalytical (Almedo, Netherlands) X-Pert Pro XRD system at 40.0 kV and 30.0 mA. It uses graphite monochromator and Cu Ka radiation to produce X-rays with a wavelength of 1.54 A °. The XRD patterns of the G0 are displayed in Figure 10 and can be found at 2= 11.83, 20.54, 27.06, 35.57, and 42.98. These match the values of Miller's indices: 020, 210, 110, 310, and 420, per ICDD File 9012230 [27]. Figure 11 displays the XRD patterns of the FeNPs that were produced. XRD analysis was used to confirm the crystalline structure of the FeNPs, revealing the typical Fe peaks at 2 = 22.80, 27.07, 32.15, 34.15, and 66.53. which, according to (JCPDS card No. 89.0950), correspond to the following values of Miller's indices: 100, 221, 141, and 442 [28]. Figure 12 displays the XRD patterns of the ZnNPs that were produced. The typical Zn peaks, which appear at 2^i = 11.14,23.41,31.75,47.53, 52.52, and 56.56, were revealed by XRD analysis, confirming the crystalline structure of the ZnNPs. These values correspond to the values of Miller's indices, which are 110, 100, 101, 311 222, and 110 according to (GCPDS card no.79-2205) [29]. Tables (1) show the crystal size values for GO, FeNPs and ZnNPs, respectively, calculated using Scherer equation.

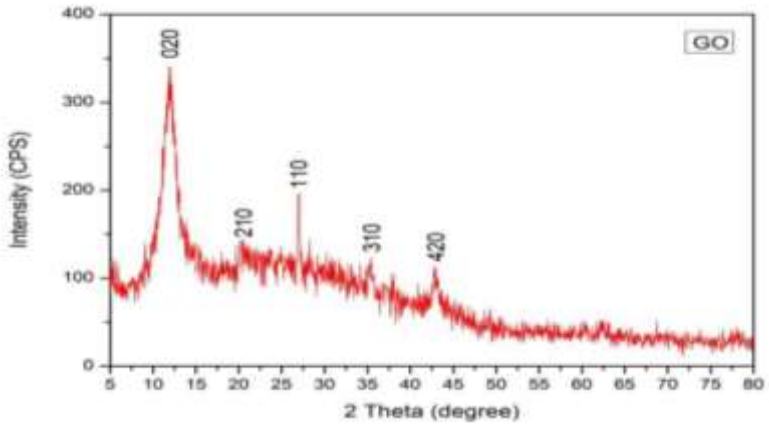


Figure 10. XRD of *Graphene Oxide*.

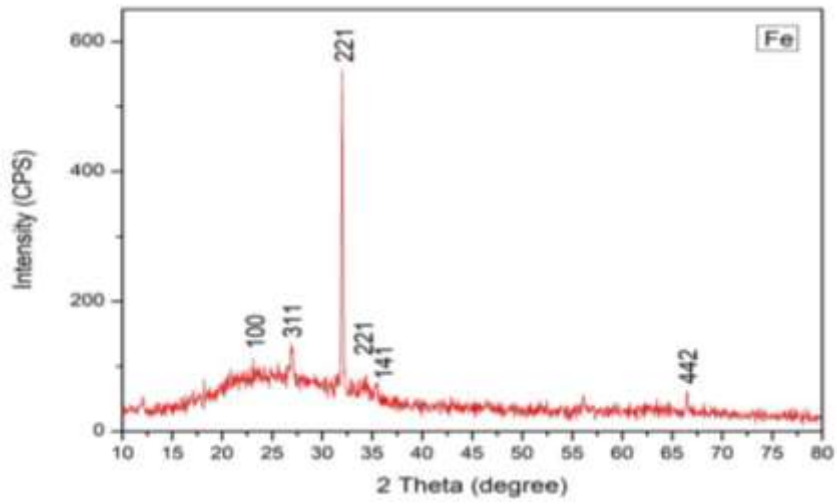


Figure 11. XRD of A- *FeNPs.*

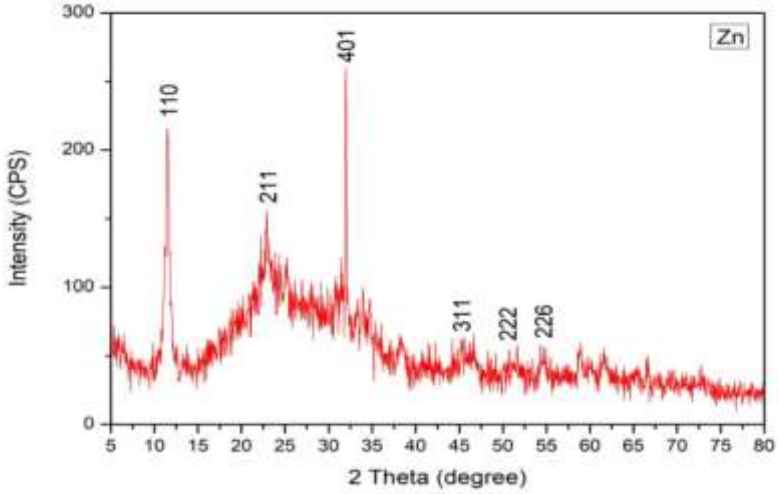


Figure 12. XRD of *ZnNPs.*

Table 1. Average and *D.average* of GO, FeNPs and MnNPs.

Element	2theta	FWHM	HKI	Average	D.average
	11.83	1.7096	020	0.8498236	
	20.54	1.0330	210	0.9673295	
GO	27.06	0.8083	110	1.9755050	1.585350
	35.57	0.8167	310	2.1405727	
	42.98	0.9750	420	1.9935450	
	22.62	0.1700	100	9.061774	
	27.07	0.2886	311	5.533418	
FeNPs	32.15	0.1473	221	11.402206	14.5737635
	34.15	0.1487	141	11.55530	
	66.53	0.1011	442	35.31611	
	11.14	0.190	110	8.161	
	23.41	0.200	100	7.753	
ZnNPs	31.75	0.165	101	10.139	20.656
	47.53	0.050	311	42.321	
	52.52	0.067	222	34.907	

4. Applications

4.1. Gas sensing measurement.

The unique electronic structure determines the conductor, semiconductor, and insulator properties of nanomaterials. Transition metal ions typically possess unfilled d-shells, allowing for reactive electronic transitions, wide band gaps, superior electrical characteristics, and high dielectric constants. As a result, Nanocomposites have exceptional and adjustable optoelectronic, optical, electrical, thermal, magnetic, catalytic, mechanical, and photochemical properties. Furthermore, Nanocomposites have a wide range of applications: sensors, fuel cells, batteries, actuators, supercapacitors, optical devices, pyroelectrics, piezoelectrics, ferroelectrics, and random access memory due to their exceptional shape and size, which manifest distinctive physicochemical properties. Potential applications also exist due to the high density of surface sites and nanostructures(30).

1-Resistance vs. operation temperature of the GO/*(Zn+Fe) NPs gas sensor using H_2S gas*.

Figure (13) represents the relationship of resistance with time at a temperature of 100 °C. At a time of (0)S, the resistance is at its highest value. After time passes, it is noted that the resistance decreases with increasing sensing time until it reaches its lowest value at a time of (65) S. When gas entry is stopped, the process is reversed and the resistance begins to increase with the calculated recovery time. It is noted that the time period for changes in resistance values is a good enough period to make this nanocomposite one of the nanocomposites that will receive attention because of its future and promise for gas sensing operations.

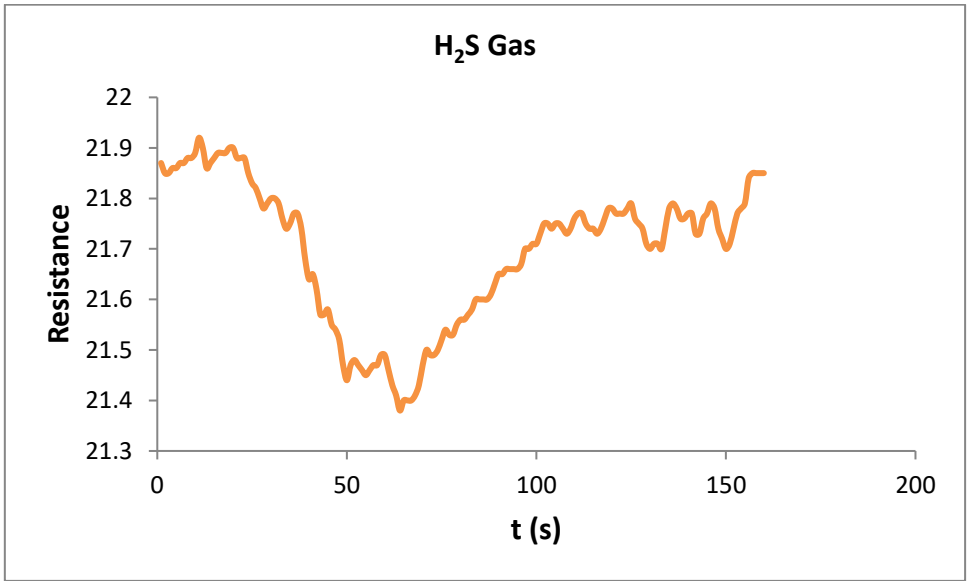


Figure 13. Resistance vs. operation temperature of the GO/*(Zn+Fe)NPs gas sensor using H_2S gas*.

2-Sensitivity vs. operating temperature of GO/(Zn+Fe) NPs *using H_2S*.

2D and 3D nanomaterials of graphene oxide and metal oxides are good sensors. The sensing value reaches a high degree despite the temperature differences. This gives the nanocomposite a high-quality sensor and sensitivity compared to graphene oxide or metal oxide when it is alone (31). The reason for this is the presence of connections largely within the surface area of the nanocomposite. Large aggregations or agglomerations occur as a result of interactions between acid groups and gas molecules, which give a high sensitivity value to the sensor due to these large aggregations on the surface of the nanocomposite. In addition to the presence of nano-metals and their oxides with graphene oxide, which works to fill all the interstitial gaps that exist between the molecules, and thus gives a large surface area for sensing the presence of gas. An increase in temperature up to 300°C does not affect the sensing and sensitivity of the nanocomposite clearly, and this is a good characteristic that gives the nanocomposite great importance for working in harsh temperature conditions.

Through the chemical interaction between the gas molecules and the active groups of the sensor, selective oxidation of volatile organic compounds occurs, and the semiconducting compound is of the P-type (32). The figure (14) shows the sensitivity % values with increasing operation temperatures.

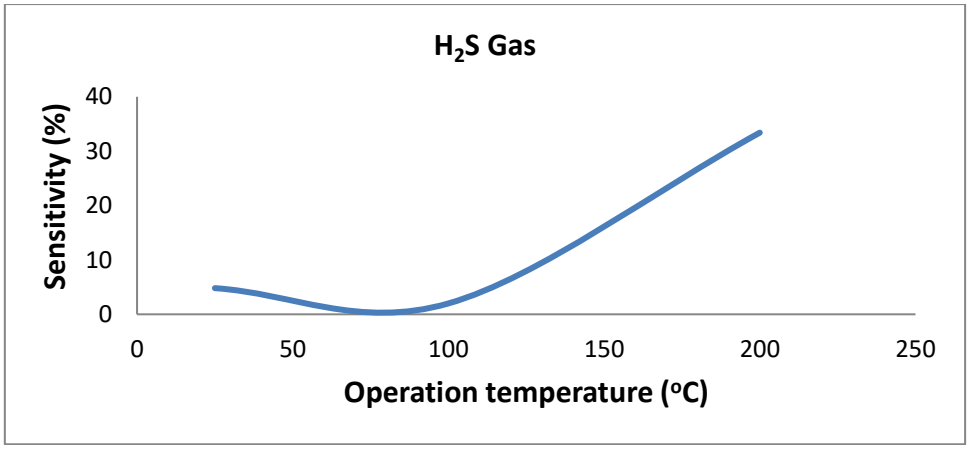


Figure 14. Sensitivity vs. operating temperature of GO/(Zn+Fe)NPs *using H_2S as gas sensing technique.*

3-Response time and Recovery time vs. operation temperature of the GO/(Zn+Fe)NPs *gas sensor using H_2S gas*.

The gas concentration has a significant impact on the response time and recovery time. As it was found that at high gas concentration, the response time is short, and this gives a good indication of the sensor used. As well as the recovery time, which is longer than the response time at high concentrations. The response time and recovery time differ from one gas to another due to the structure and composition of the gas itself and its effect on the membrane made from the sensor in terms of thickness and surface area, as well as the quality of the membrane and the active groups it contains.

Response time and recovery time are of real importance in determining the quality of the sensor. In terms of rapid response to any gas leak in record time. The high selectivity of sensor selection under different conditions must be taken into account. On this basis, each gas has its own conditions in terms of composition, structure, concentration, and the type of membrane on which it works. Here the temperature had little effect up to 300°C. the greatest response time (12.7) at a temperature of 200 °C. At 25 degrees Celsius, the lowest response time is (10.9). The recover time values are (148) at 25 °C, which is represented by series 2, orange, and (93.5) at 200 °C. Increased oxygen adsorption on the surface depletes the near-surface region of conduction electrons, resulting in an electron-depleted surface layer.

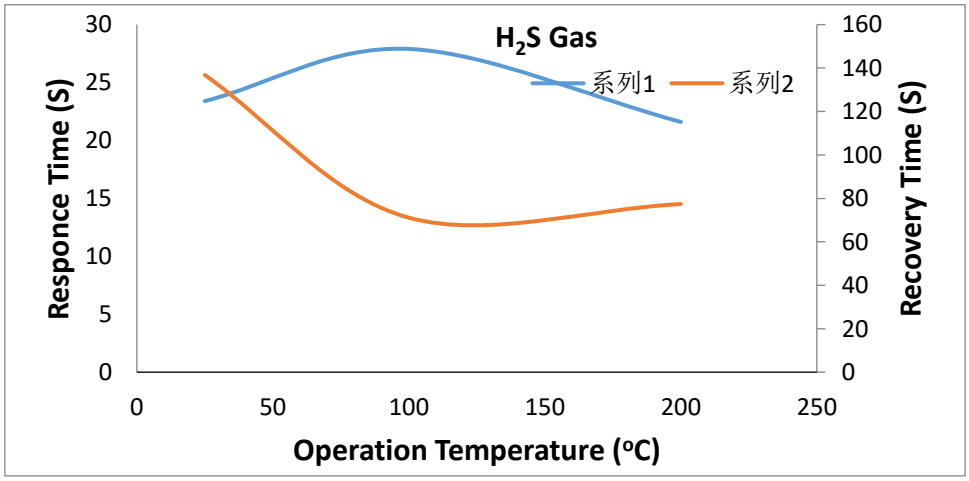


Figure 15. Response time and Recovery time vs. operation temperature of the GO/(Zn+Fe)NPs *gas sensor using H_2S gas*.

5. Conclusion

This study aims to develop and improve nanosensors in line with evolving scientific realities and to achieve the highest technical specifications. Future objectives include finding suitable solutions to reduce environmental pollution by placing sensors in relevant locations. Furthermore, ongoing research will focus on developing and addressing shortcomings to provide the best possible scientific service to our community. The applications of H2S gases were used on the prepared complexes of graphene oxide, Iron and Manganese nanoparticles GO/(Zn+Fe)NPs). These composites have given a good response by the gases at normal temperatures. In addition, these composites can also respond at temperatures up to 250°C. It is noted through the practical results that there is a discrepancy in the values of resistance (increase or decrease in its value) compared to temperatures. These composites can be at the forefront of materials that are used in gas detection and sensitivity in different conditions of temperatures. The danger resulting from the spread of these gases can be avoided at the beginning of its occurrence process temperatures. These composites have a specificity in response, and this is what was observed from the values of response time and recovery time against operation temperatures. In addition to the relative sensitivity values and the wide range of these values against operating temperatures. This makes them well-used sensors in the field of gas detection. The research relies on simple and inexpensive methods for preparing nanosensors compared to research that dealt with the same content.

Acknowledgments

Thanks, appreciation, and gratitude to the College of Science and the Department of Chemistry at the Anbar University for providing the necessary equipment and laboratories for its researchers and following them up through continuous supervision of the completion of scientific research. Thanks and appreciation to the Iraqi Journal of Science in the College of Science, University of Baghdad. The ratio used in preparing the composite is 10:1, which covers the surface area-to-weight ratio of both materials, such that the metal concentration completely covers the surface area of the graphene oxide.

Conflict of interest

The author declares no conflict of interest.

References

1. Okpala, C. C. The benefits and applications of nanocomposites. *Int. J. Adv. Eng. Tech*, *12*, 18. (2014).
2. Clyne, T. W., & Hull, D. An introduction to composite materials. Cambridge University press (2019).
3. Malik, S., Muhammad, K., & Waheed, Y. Nanotechnology: A revolution in modern industry. *Molecules*, *28*(2), 661. (2023).
4. Singh, N. B., & Agarwal, S. Nanocomposites: an overview. *Emerging Materials Research*, *5*(1), 5-43. (2016).
5. Pandey, N., Shukla, S. K., & Singh, N. B. Water purification by polymer nanocomposites: an overview. *Nanocomposites*, *3*(2), 47-66. (2017).
6. T. Kuilla, S. Bhadra, D. Yao, N.H. Kim, S. Bose, J.H. Lee, Recent advances in graphene based polymer composites, Prog. Polym. Sci. 35 (11) 1350–1375. (2010).
7. Y. Cui, S.I. Kundalwal, S. Kumar, Gas Barrier Performance of Graphene/polymer Nanocomposites, Pergamon, pp. 313–333. 2016.
8. F. Pendolino, N. Armata, Graphene Oxide in Environmental Remediation Process, 2017.
9. Smith, A. T., LaChance, A. M., Zeng, S., Liu, B., & Sun, L. Synthesis, properties, and applications of graphene oxide/reduced graphene oxide and their nanocomposites. *Nano Materials Science*, *1*(1), 31-47. (2019).
10. Jiříčková, A., Jankovský, O., Sofer, Z., & Sedmidubský, D. Synthesis and applications of graphene oxide. *Materials*, *15*(3), 920. (2022).
11. Mousavi, S. S., & Karami, A. Graphene Oxide from Natural Products and Its Applications in the Agriculture and Food Industry. In *Graphene from Natural Sources* (pp. 95-116). CRC Press. (2022).
12. Li, F.; Jiang, X.; Zhao, J.; Zhang, S. Graphene oxide: A promising nanomaterial for energy and environmental applications. Nano Energy, 16, 488–515. 2015.

13. Palencia, M., & García-Quintero, A. Green synthesis of nanomaterials and their use in bio-and nanoremediation. In *Bio and Nanoremediation of Hazardous Environmental Pollutants* (pp. 195-229). CRC Press. (2023).
14. T.A. Dontsova, S.V Nahirniak, I.M. Astrelin, Review article metaloxide nanomaterials and nanocomposites of ecological purpose, 2019.
15. Bijesh, P., Selvaraj, V., & Andal, V. A review on synthesis and applications of nano metal Oxide/porous carbon composite. *Materials Today: Proceedings*, *55*, 212-219. (2022).
16. Ho, S. H., Zhu, S., & Chang, J. S. Recent advances in nanoscale-metal assisted biochar derived from waste biomass used for heavy metals removal. *Bioresource technology*, *246*, 123-134. (2017).
17. Ramesh, M., Janani, R., Deepa, C., & Rajeshkumar, L. Nanotechnology-enabled biosensors: A review of fundamentals, design principles, materials, and applications. *Biosensors*, *13*(1), 40. (2022).
18. Motamedi, E., Atouei, M. T., & Kassaee, M. Z. Comparison of nitrate removal from water via graphene oxide coated Fe, Ni and Co nanoparticles. *Materials Research Bulletin*, *54*, 34-40. (2014).
19. Abdelrahman, A., Erchiqui, F., Nedil, M., & Mohamed, S. Enhancing fluidic polymeric solutions' physical properties with nano metals and graphene additives. *Journal of Molecular Liquids*, *370*, 121052. (2023).
20. Liu, X., Chen, S., Zhang, Y., Liu, M., Emori, W., & Shao, Y. Preparation of graphene oxide–boron nitride hybrid to reinforce the corrosion protection coating. *Corrosion Reviews*, *39*(2), 123-136. (2021).
21. Fanelli, F., & Fracassi, F. Aerosol-assisted atmospheric pressure cold plasma deposition of organic–inorganic nanocomposite coatings. *Plasma Chemistry and Plasma Processing*, *34*(3), 473-487. (2014).
22. Revathi, B., Perumal, P., & Deivamani, D. Optical and Gas Sensing Properties of Pr-Doped TiO2 Thin Film. *Iranian Journal of Materials Science and Engineering*, *20*(2). (2023).
23. He, Q., Liu, J., Zhang, M., Zhai, Z., & Jiang, B. Molecular Dynamics Simulation on the effect of self-resistance electric heating on carbon fiber surface chemical properties and fiber/PP interfacial behavior. *Polymers*, *14*(5), 1043. (2022).
24. Wahyono, T., Astuti, D. A., Wiryawan, I. K. G., Sugoro, I., & Jayanegara, A. Fourier transform mid-infrared (FTIR) spectroscopy to identify tannin compounds in the panicle of sorghum mutant lines. In *IOP Conference Series: Materials Science and Engineering* (Vol. 546, No. 4, p. 042045). IOP Publishing. (2019, June).
25. Batool, F., Iqbal, M. S., Khan, S. U. D., Khan, J., Ahmed, B., & Qadir, M. I. Biologically synthesized iron nanoparticles (FeNPs) from Phoenix dactylifera have anti-bacterial activities. *Scientific Reports*, *11*(1), 22132. (2021).
26. Radini, I. A., Hasan, N., Malik, M. A., & Khan, Z. Biosynthesis of iron nanoparticles using Trigonella foenum-graecum seed extract for photocatalytic methyl orange dye degradation and antibacterial applications. *Journal of Photochemistry and Photobiology B: Biology*, *183*, 154-163. (2018).
27. Hidayah, N. M. S., Liu, W. W., Lai, C. W., Noriman, N. Z., Khe, C. S., Hashim, U., & Lee, H. C. Comparison on graphite, graphene oxide and reduced graphene oxide: Synthesis and characterization. In *AIP Conference Proceedings* (Vol. 1892, No. 1, p. 150002). AIP Publishing LLC. (2017, October).
28. Radini, I. A., Hasan, N., Malik, M. A., & Khan, Z. Biosynthesis of iron nanoparticles using Trigonella foenum-graecum seed extract for photocatalytic methyl orange dye degradation and antibacterial applications. *Journal of Photochemistry and Photobiology B: Biology*, *183*, 154-163. (2018).
29. Manyasree, D., Kiranmayi, P., & Venkata, R. K. Characterization and antibacterial activity of ZnO nanoparticles synthesized by co-precipitation method. *Int J App Pharm*, *10*(6), 224-8. (2018).
30. Yoon, Y., Truong, P. L., Lee, D., & Ko, S. H. Metal-oxide nanomaterials synthesis and applications in flexible and wearable sensors. *ACS Nanoscience Au*, *2*(2), 64-92. (2021).
31. Kosmaca, J., Katkevics, J., Andzane, J., Sondors, R., Jasulaneca, L., Meija, R., ... & Erts, D. Humidity-dependent electrical performance of CuO nanowire networks studied by electrochemical impedance spectroscopy. *Beilstein Journal of Nanotechnology*, *14*(1), 683-691. (2023).
32. Cheng, L., Li, Y., Sun, G., Cao, J., & Wang, Y. In-situ growth of CdS QDs on ZnO porous microrods for highly sensitive detection of TEA at lower temperature. *Vacuum*, *212*, 112003. (2023).